Studies of field-induced nonequilibrium electron transport in an In x Ga 1x N (x0.6) epilayer grown on GaN

W. Liang, K. T. Tsen, D. K. Ferry, K. H. Kim, J. Y. Lin, and H. X. Jiang

Citation: Applied Physics Letters **82**, 1413 (2003); doi: 10.1063/1.1556576
View online: http://dx.doi.org/10.1063/1.1556576
View Table of Contents: http://scitation.aip.org/content/aip/journal/apl/82/9?ver=pdfcov
Published by the AIP Publishing

Studies of field-induced nonequilibrium electron transport in an $In_xGa_{1-x}N$ ($x \cong 0.6$) epilayer grown on GaN

W. Liang and K. T. Tsen[a)]
Department of Physics and Astronomy, Arizona State University, Tempe, Arizona 85287

D. K. Ferry
Department of Electrical Engineering, Arizona State University, Tempe, Arizona 85287

K. H. Kim, J. Y. Lin, and H. X. Jiang
Department of Physics, Kansas State University, Manhattan, Kansas 66506

(Received 25 October 2002; accepted 2 January 2003)

Field-induced electron transport in an $In_xGa_{1-x}N$ ($x \cong 0.6$) sample grown on GaN has been studied by subpicosecond Raman spectroscopy. Nonequilibrium electron distribution and electron drift velocity due to the presence of piezoelectric and spontaneous fields in the $In_xGa_{1-x}N$ layer have been directly measured. The experimental results are compared with ensemble Monte Carlo calculations and reasonable agreements are obtained.
[DOI: 10.1063/1.1556576]

Gallium nitride (GaN), aluminum nitride (AlN), indium nitride (InN), and their alloys, have long been considered as very promising materials for device applications.[1,2] Semiconductor alloys such as $In_xGa_{1-x}N$ have been successfully used in the fabrication of blue-green light emitting diodes and laser diodes.[2–7] Recently, growth of high-quality InN as well as $In_xGa_{1-x}N$ have been demonstrated.[8–10] The next natural step is to manufacture high-performance InN and $In_xGa_{1-x}N$ electronic devices. In order to improve the design of these devices, knowledge of their electron transport properties is indispensable. In this letter, we report experimental results on subpicosecond Raman studies of electric field-induced electron transport in an $In_xGa_{1-x}N$ ($x \cong 0.6$) sample grown on GaN.

The Si-doped $In_xGa_{1-x}N$ epilayer of about 0.15 μm thickness used in this work was grown on top of a 1.5 μm GaN epilayer by metal organic chemical vapor deposition. Prior to the GaN growth, a 25-nm-thick GaN buffer layer was grown on *c*-plane sapphire at 550 °C. Subsequent epilayer growth was carried out at 1050 °C for GaN and 710 °C for $In_xGa_{1-x}N$. Trimethylgallium (TMGa) and trimethylindium (TMIn) were used as the precursors. Nitrogen and hydrogen were used as carrier gases for $In_xGa_{1-x}N$ and GaN, respectively. High-purity ammonia was used as the active nitrogen source. To vary In content in $In_xGa_{1-x}N$, the TMIn flow rate was varied while other growth parameters were fixed. The $In_xGa_{1-x}N$ epilayer was doped by Si at a flow rate of 0.25 sccm of 10 ppm silane to improve the materials quality as well as to enhance the emission efficiency. GaN and $In_xGa_{1-x}N$ growth rate were 3.6 and 0.3 μm/h, respectively. The typical room-temperature electron concentration and mobility of $In_xGa_{1-x}N$ alloy are $2\times10^{17}\ \mathrm{cm}^{-3}$ and 160 cm^2/V s, respectively, as determined by Hall effect measurements.

The output of the second harmonic of a cw mode-locked YAlG laser is used to synchronously pump a dual-jet R6G dye laser. The dye laser, which has a pulse width of FWHM$\cong$0.6 ps, photon energy of $\hbar\omega \cong 2.17$ eV, a repetition rate of 76 MHz, was used to both excite and probe the $In_xGa_{1-x}N$ sample. In our transient experiments, since the same laser pulse is used to excite and probe nonequilibrium electron transport, the experimental results represent an average over the duration of the laser pulse. The single-particle scattering (SPS) spectra were taken in the $Z(X,Y)\bar{Z}$ scattering configuration where $X=(100)$, $Y=(010)$, and $Z=(001)$ so that only the SPS spectra associated with spin-density fluctuations were detected.[11] The backward-scattered Raman signal is collected and analyzed by a standard Raman system consisting of a double spectrometer, a photomultiplier tube. All the data reported here were taken at $T=300$ K.

Figure 1 shows a typical photoluminescence spectrum for an $In_xGa_{1-x}N$ sample. This E_0 band-gap luminescence of $In_xGa_{1-x}N$ sample peaks at about 1.90 eV and has a FWHM of about 0.2 eV. Comparison of the spectrum with Refs. 8, 9, and 10 shows that our sample is of good quality and has an In concentration of about $x \cong 0.6$.

Figure 2(a) shows a typical SPS spectrum for an $In_xGa_{1-x}N$ ($x \cong 0.6$) sample taken at $T=300$ K and for an

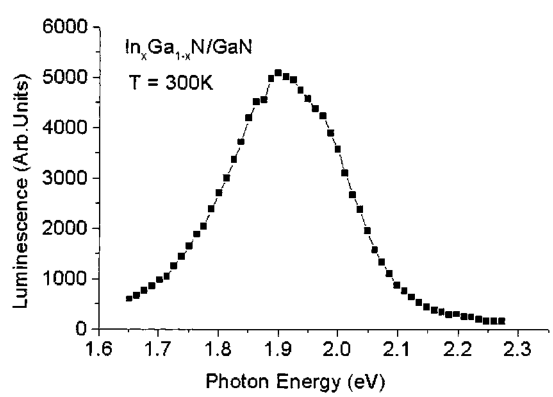

FIG. 1. Typical electron–hole pair luminescence spectrum for an $In_xGa_{1-x}N$/GaN sample. The photon energy of excitation laser is $\hbar\omega \cong 2.17$ eV. We deduce that In concentration in the sample is about $x=0.6$ by comparing the data with those of Refs. 8, 9, and 10.

[a)]Electronic mail: tsen@asu.edu

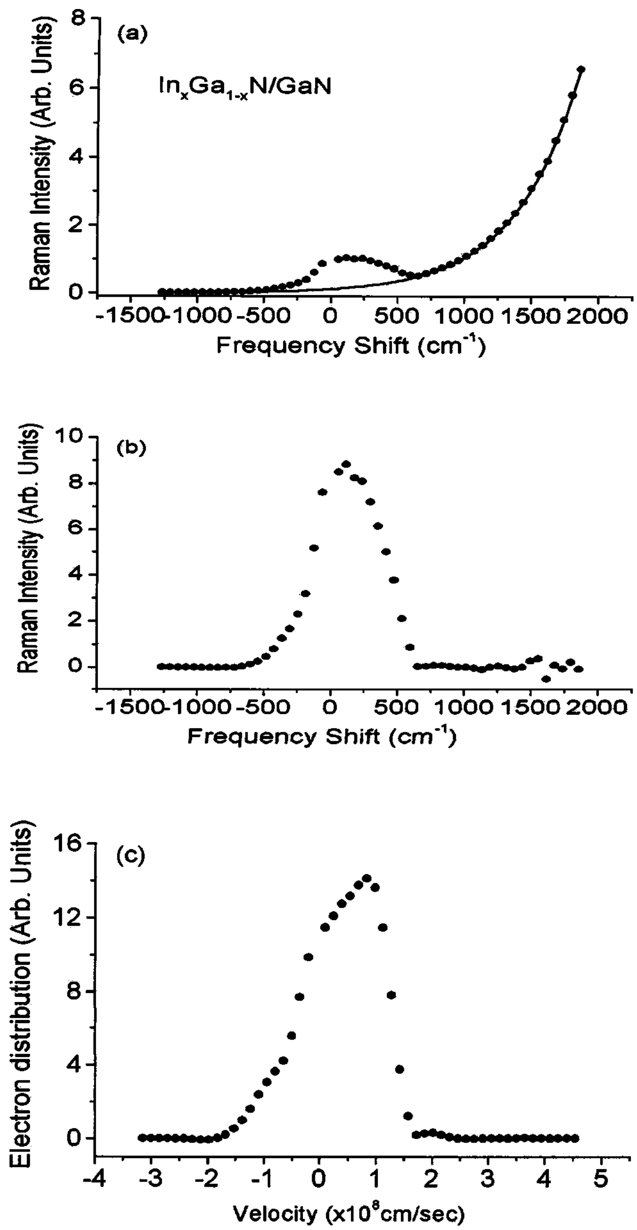

FIG. 2. (a) Typical SPS spectrum taken at $T=300$ K and a photoexcited electron–hole pair density of $n \cong 1\times10^{18}$ cm^{-3}. The SPS spectrum is found to lie on top of a luminescence background (solid curve) that can be fit very well by an exponential curve; (b) SPS spectrum after the subtraction of the luminescence background; and (c) electron distribution function obtained from (b).

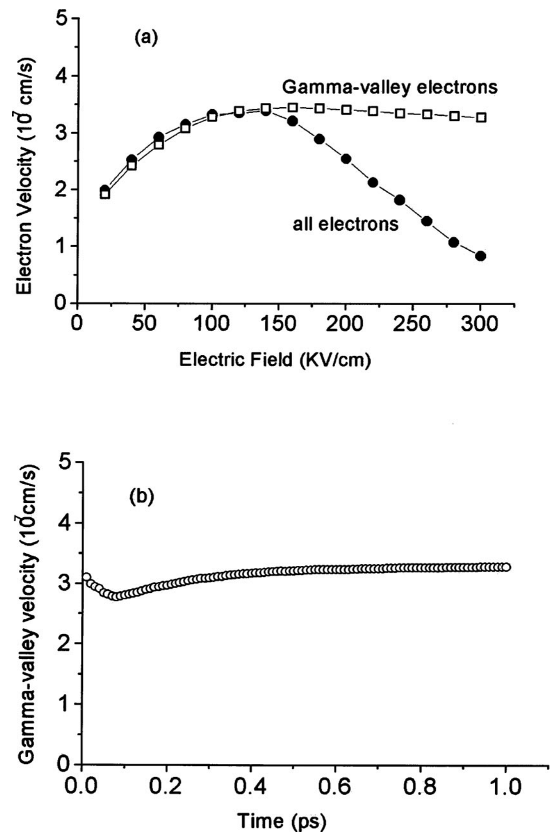

FIG. 3. Ensemble Monte Carlo simulation for an $In_xGa_{1-x}N$ ($x=0.6$) sample at $T=300$ K. (a) electron velocity as a function of the applied electric field intensity for Γ-valley electrons (open squares) and all electrons (filled circles), as indicated; (b) Γ-valley electron velocity as a function of time.

electron–hole pair density of $n \cong 1\times10^{18}$ cm^{-3}. The SPS spectrum sits on a smooth background coming from the luminescence of E_0 band gap of $In_xGa_{1-x}N$. Similar to previous studies on other III–V semiconductors such as GaAs, this background luminescence has been found to be fit very well by an exponential function.[12–14] The SPS spectrum is obtained by subtracting Fig. 2(a) from this luminescence background. Following the procedure described in detail in Ref. 13, this subtracted spectrum [Fig. 2(b)] can then be very easily transformed to electron distribution function. The electron distribution thus obtained is shown in Fig. 2(c). The intriguing feature worthwhile pointing out is that the electron distribution function has been found to shift toward the wavevector transfer **q** direction—an indication of the presence of an electric field **E** parallel to $-\mathbf{q}$. The electron distribution has a cutoff velocity of around 1.5×10^8 cm/s, indicative of the band structure effects and the onset of electron intervalley scattering processes in $In_xGa_{1-x}N$. The electron drift velocity deduced from the measured electron distribution [Fig. 2(c)] is found to be $V_d \cong (3.8\pm0.4)\times10^7$ cm/s.

We have also carried out an ensemble Monte Carlo (EMC) simulation[15] for the transport of the photoexcited carriers in $In_xGa_{1-x}N$. Here, we treat polar optical phonon, acoustic phonons, intervalley phonons, and dislocation scattering. For dislocation scattering,[16,17] we assumed that a defect density of $10^8/\mathrm{cm}^2$ existed in the $In_xGa_{1-x}N$ layer; however, it is found that because of the presence of much more efficient inelastic scattering processes, this elastic defect scattering process can affect the low field mobility but is not important for the high-field transient experiments carried out here. Disorder-induced scattering due to In concentration fluctuations in $In_xGa_{1-x}N$ is not included in the EMC simulation because it is an elastic scattering process that does not affect the high field transport.[15] Within the Γ valley, which is the valley measured in the experiment, the high-field behavior is dominated by polar optical phonon scattering. In Fig. 3(a), we plot the velocity-field relationship for these carriers. The peak in the velocity occurs at around 150 kV/cm, beyond which carriers begin to rapidly transfer to the satellite valley. Nevertheless, even the carriers that remain in the Γ valley appear to show the onset of saturation and a weak negative differential resistance, both of which are due to this type of scattering in a non-parabolic band. In Fig. 3(b), we plot the transient velocity of the Γ valley electrons at 200 kV/cm. Their initial velocity is determined by the excess energy of the photon excitation within the band. This gives rise to a nonzero velocity, as only a hemisphere (in momentum space) of carriers is excited at the surface. This directed velocity rapidly drops, and the field-induced rise follows. We note that there is very little, if any, overshoot in the carrier velocity, which is a result of the fact that polar scattering is much better in relaxing energy than momentum. We notice that the EMC results are in reasonable agreement with the experimental values quoted above.

There have been experimental evidences[18–21] that an extremely large (of the order of MV/cm) electric field exists in the layer of $In_xGa_{1-x}N$ in the $GaN/In_xGa_{1-x}N/GaN$ structures as a result of huge lattice mismatch between $In_xGa_{1-x}N$ and GaN. We believe that, similar to the previous studies, the source of high electric field in the $In_xGa_{1-x}N/GaN$ sample studied in this work arises from a combination of the polarization field and the piezoelectric field. Although the direction of the net electric field is indicated in the shift of measured electron distribution (in this case, the net field points from GaN to $In_xGa_{1-x}N$ layers), the agreement between the experiment and the simulation is not sufficiently good to make a quantitative estimate of this field. Nevertheless, we can estimate the polarization field to be about 2.8 MV/cm, whereas the piezoelectric field is estimated to be some 50% smaller, although we do not have a good measure of the piezo-electric constants in this alloy.[22,23] We have extrapolated from the InN and GaN values, and this is not expected to be particularly accurate.

In conclusion, we have studied field-induced electron transport in an $In_xGa_{1-x}N$ ($x \cong 0.6$) sample grown on GaN by subpicosecond Raman spectroscopy. Nonequilibrium electron distribution and electron drift velocity due to the presence of piezoelectric and spontaneous fields in the $In_xGa_{1-x}N$ layer have been directly measured. The experimental results are compared with ensemble Monte Carlo calculations and reasonable agreements are obtained.

1. S. Strite and H. Morkoc, J. Vac. Sci. Technol. B **10**, 1237 (1992).
2. S. N. Mohammad and H. Morkoc, Prog. Quantum Electron. **20**, 361 (1996).
3. S. Nakamura, M. Senoh, N. Iwasa, and S. Nagahama, Jpn. J. Appl. Phys., Part 2 **34**, L797 (1995).
4. S. Nakamura, M. Senoh, N. Iwasa, S. Nagahama, T. Yamada, and T. Mukai, Jpn. J. Appl. Phys., Part 2 **34**, L1332 (1995).
5. S. Nakamura, M. Senoh, S. Nagahama, N. Iwasa, T. Yamada, T. Matsushita, H. Kiyoku, and Y. Sugimoto, Jpn. J. Appl. Phys., Part 2 **35**, L74 (1996).
6. L. J. Mawst, A. Bhattacharya, J. Lopez, D. Botez, D. Z. Garbuzov, L. De-Marco, J. C. Connolly, M. Jansen, F. Fang, and R. Nabiev, Appl. Phys. Lett. **69**, 1532 (1996).
7. E. Gregger, K. H. Gulden, P. Riel, H. P. Schweizer, M. Moser, G. Schmiedel, P. Kiesel, and G. H. Dohler, Appl. Phys. Lett. **68**, 2383 (1996).
8. J. Wu, W. Walukiewicz, K. M. Yu, J. W. Ager III, E. E. Haller, Hai Lu, W. J. Schaff, Y. Saito, and Y. Nanishi, Appl. Phys. Lett. **80**, 3967 (2002).
9. J. Wu, W. Walukiewicz, K. M. Yu, J. W. Ager III, E. E. Haller, Hai Lu, and W. J. Schaff, Appl. Phys. Lett. **80**, 4741 (2002).
10. T. Matsuoka, H. Okamoto, M. Nakao, H. Harima, and E. Kurimoto, Appl. Phys. Lett. **81**, 1246 (2002).
11. M. V. Klein, in *Light Scattering in Solids I*, edited by M. Cardona (Springer, New York, 1983), Vol. 8, p. 151.
12. D. S. Kim and P. Y. Yu, Phys. Rev. B **43**, 4158 (1991).
13. E. D. Grann, K. T. Tsen, D. K. Ferry, A. Salvador, A. Botcharev, and H. Morkoc, Phys. Rev. B **53**, 9838 (1996).
14. E. D. Grann, S. J. Sheih, K. T. Tsen, O. F. Sankey, S. E. Guncer, D. K. Ferry, A. Salvador, A. Botcharev, and H. Morkoc, Phys. Rev. B **51**, 1631 (1995).
15. For a review of ensemble Monte Carlo simulation, see, for example, D. K. Ferry, *Semiconductor Transport* (Taylor & Francis, London, 2000), Chap. 4.
16. N. G. Weimann, L. F. Eastman, D. Doppulapudi, H. M. Ng, and T. D. Moustakas, J. Appl. Phys. **83**, 3656 (1998).
17. D. Jena, A. C. Gossard, and U. K. Mishra, Appl. Phys. Lett. **76**, 1707 (2000).
18. M. R. McCartney, F. A. Ponce, J. Cai, and D. P. Bour, Appl. Phys. Lett. **76**, 3055 (2000).
19. D. Cherns, J. Barnard, and F. A. Ponce, Solid State Commun. **111**, 281 (1999).
20. T. Takeuchi, S. Sota, M. Katsuragawa, M. Komori, H. Takeuchi, H. Amano, and I. Akasaki, Jpn. J. Appl. Phys., Part 2 **36**, L382 (1997).
21. T. Takeuchi, C. Wetzel, S. Yamaguchi, H. Sakai, H. Amano, and I. Akasaki, Appl. Phys. Lett. **73**, 1691 (1998).
22. F. Bernardini, V. Fiorentini, and D. Vanderbilt, Phys. Rev. B **56**, R10024 (1997).
23. T.-H. Yu and K. F. Brennan, J. Appl. Phys. **89**, 3827 (2001).